Open Access **Baghdad Science Journal** **P-ISSN: 2078-8665**
Published Online First: July 2021 **2022, 19(1): 132-140** **E-ISSN: 2411-7986**

DOI: http://dx.doi.org/10.21123/bsj.2022.19.1.0132

Kinetic, Isotherm, and Thermodynamic Study of Bismarck Brown Dye Adsorption onto Graphene Oxide and Graphene Oxide-Grafted-Poly (n-butyl methacrylate-co-methacrylic Acid)

***Alaa A. Mizhir*[1]** ***Hadi S. Al-Lami*[2*]** ***Ali A. Abdulwahid*[2]**

[1]Department of Applied Marine Science, Faculty of Marine Science, University of Basrah, Basrah, Iraq
[2]Department of Chemistry, College of Science, University of Basrah, Basrah, Iraq
[*]Corresponding author: allbahily79@yahoo.com , hadisalma54@yahoo.com [*], alirazaq2013@yahoo.com
[*]ORCID ID: https://orcid.org/0000-0002-7608-1500 , https://orcid.org/0000-0001-8716-6385 [*], https://orcid.org/0000-0001-5639-4297

Received 19/4/2020, Accepted 10/13/2020, Published Online First 20/7/2021, Published 1/2/2022

Abstract:

The adsorption behavior of Bismarck brown (BB) dye from aqueous solutions onto graphene oxide GO and graphene oxide-g-poly (n-butyl methacrylate-co-methacrylic acid) GO-g-pBCM as adsorbents was investigated. The prepared GO and GO-g-pBCM were characterized by Fourier transform infrared spectroscopy FTIR, which confirmed the compositions of the prepared adsorbents. Adsorption of BB dye onto GO and GO-g-pBCM was explored in a series of batch experiments under various conditions. The data were examined utilizing Langmuir and Freundlich isotherms. The Langmuir isotherm was seen as increasingly reasonable from the experimental information of dye on formulating adsorbents. Kinetic investigations showed that the experimental data were fitted very well to the pseudo-second-order model, and the calculated positive values of the (ΔH° and ΔS°) indicated that the adsorption of BB dye onto GO and GO-g-pBCM was endothermic and increasing of the adsorption process randomness. The negative values of (ΔG°) imply that the adsorption process was spontaneous.

Key words: Adsorption isotherm, Bismarck brown, Freundlich, Graphene oxide, Langmuir, Pseudo-second-order model.

Introduction

Water contamination is one of the greatest dangers confronting humankind, which is ascribed to the fast industrialization and has been a significant subject of research overall [1]. Organic and synthetic dyes, the contaminant effluents cleared from different food and fabric industries, are one of the key sources of environmental contamination owed to their non-biodegradable behavior [2]. The enormous amount of industrialized organic dyes is discharged by the textile industry into waterways and other water resources, which eventually spoil water quality [3]. The vast majority of the manufactured dyes contain complex structures having azo groups, exhibit serious harmfulness when breathed in utilizing drinking dye-contaminated water, which in the end causes cancers of various portions of the human body [4]. Hence, the exclusion of dyes from wastewater is basic for a more protected environment. Different techniques have been accounted for in the literature for the clearing of dyestuffs, including photocatalysis and adsorption [5].

Some approaches have been proven to expel dyes from wastewater, for example, flocculation, and ultra-filtration, precipitation, and so on. These procedures are costly and don't eliminate the color which prompts other contamination issues [6]. Because of these downsides, the expulsion of color from nature has faced more challenges. Adsorption is as yet a favored technique by investigators on account of its easy procedure, high effectiveness, simple recuperation, and adaptability. Moreover, the adsorbent can be reused many times and the risky byproducts produced through degradation can be removed [7].

Graphene oxide (GO), presents excellent adsorbent performance for heavy metals, dyes, and pharmaceutical antibiotics because of the abundant oxygen-containing functional groups on the two-dimensional 2D large surface, such as hydroxyl,

carboxyl, and epoxy groups [8]. These oxygen-containing functional groups not only can complex pollutants in wastewater but also provide the reactive sites of chemical reactions for functionalizing graphene oxide [9]. Functionalization of GO composites using small molecules [10] or polymers containing abundant carboxylic groups like poly (acrylic acid) and other analog polymers [11], which have a strong affinity to most positively, charged organic pollutants and the ability to enhance water dispersibility. Recently, numerous researches have been carried out to explore the environmental applications of GO and GO-based composite adsorbents, and these composite materials revealed outstanding adsorption capacities against various toxic compounds in an aqueous solution [12].

Herein, we report for using the prepared graphene oxide (GO) and graphene oxide-g-poly (n-butyl methacrylate-co-methacrylic acid) (GO-g-pBCM) as adsorbents for removal of Bismarck Brown (BB) dye from wastewater by adsorption process. The current research work will explore the mechanism of adsorption and adsorption kinetics of the dye. The adsorption isotherms will be designated by using Langmuir and Freundlich isotherms. Further, this paper also discusses various thermodynamic parameters such as Gibbs free energy change (ΔG°), the heat of adsorption (ΔH°) and entropy change (ΔS°) respectively.

Materials and Methods:

All chemicals utilized are of the reagent grades. They were purchased from Sigma-Aldrich Company and used without any further treatment.

Branson Ultrasonic™, Type DHA-1000, Fisher Scientific (USA) and basic 20 pH-meter, Type E-08328 Alella-Barcelona, with a combined glass electrode, Crison Instruments, S. A. (EU) were used in the preparation and adsorption experiments.

Infrared spectra of the GO and GO-g-PBCM composite were recorded on Shimadzu, FTIR-8400S spectrometer/Japan as KBr pellets in the region 400-4000 cm^{-1} to investigate the chemical structure. The absorbance intensity of BB was recorded over the range of 200-800 nm on a PG Instruments Limited, model, T80 (EMC-LAB) a UV-Visible spectrophotometer/Germany using quartz cell of 1cm length at λ_{max} 457 nm.

Synthesis of Graphene Oxide (GO)

GO was prepared by a modified Hummers method [13]. 2.0 g graphite powder and 1.0 g $NaNO_3$ were dissolved in 46.0 mL H_2SO_4 (98%) under an ice bath. The mixture was left with stirring for 15 min, and then 6.0 g $KMnO_4$ was gradually added to the suspension with lowering the stirring speed as conceivable to control the temperature below 20°C. The suspension was left stirring for an additional 2 hrs. Afterward, 100.0 mL of deionized water was added to the suspension with raising the controlled temperature, and it ought to be limited lower than 98°C. After 15 min, the suspension was then additionally diluted to 280.0 mL with warm deionized water and 20.0 mL H_2O_2 (30%), thus causing changing the suspension color to bright yellow. At that point, the suspension was filtered and washed with a warm aqueous 5% HCl solution and deionized water, separately, until no sulfate was found, and the pH of the filtrate was adjusted to 7.0. The GO was dried under vacuum at 50°C.

Copolymerization of n-butyl methacrylate/methacrylic acid (pBCM)

Butyl methacrylate monomer (BM) was washed twice with 5% NaOH to remove inhibitor and twice with water, then it was dried over anhydrous $MgSO_4$, then with calcium hydride, and freshly vacuum distilled before copolymerization. Methacrylic acid monomer (MAA) was distilled under reduced pressure before use in the copolymerization using benzoyl peroxide (Bz_2O_2) as an initiator. The copolymerization was carried out in the round bottom flask of equimolar amounts of freshly distilled n-butyl methacrylate and methacrylic acid under dry N_2 gas in a water bath after adding benzoyl peroxide ($1x10^{-4}$ mole/L) at 70℃ [13,14]. The copolymer was precipitated into methanol. It was vacuum dried at room temperature after the filtration and washing with methanol.

Synthesis of Graphene Oxide-poly (n-butyl methacrylate-co-methacrylic acid) (GO-g-pBCM)

The GO-g-pBCM composite was obtained by grafting polymerization. pBCM (0.3 g) and EDC (1-ethyl-3-(3-dimethylaminopropyl)-carbodiimide hydrochloride) (0.03 g) was added to the GO (0.3 g) dispersed in (7.5 mL) of phosphate buffer solution and the reaction mixture was sonicated for (30 min.). Then, it was left with stirring for 24 hrs. at room temperature. Finally, the formed composites were separated, washed with DI water over three times, and dried as a dark grey powder for 24 hrs. under vacuum [15].

Preparation of Aqueous Dye Solution

Bismarck Brown BB (FW=419.31) was used without any purification in this study, and its chemical structure is shown in Fig. 1. A stock solution of the dye 1000.0 mg/L was prepared for the adsorption experiments and then the required

concentrations were provided with the dilution by using deionized water.

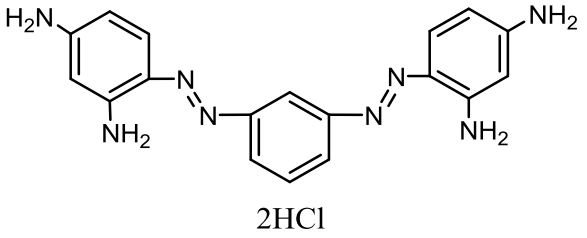

Figure 1. Chemical structure of Bismarck Brown BB [16].

Batch Experiments

The adsorption process was done using a 0.1L of dye solution with an initial concentration of 400.0 mg/L as an initial concentration of adsorbents GO and GO-g-pBCM by contacting a 25.0 mg as a fixed weight of adsorbents for each of the initial concentrations, and the solutions were shaken at 200 rpm for 24 hrs. at 27℃. The equilibrium concentration was determined at λ_{max} 457 nm for BB dye by using a UV-Visible Spectrophotometer.

The amounts of adsorbed dyes per gram of adsorbents GO and GO-g-pBCM (q_e) on the prepared adsorbents was calculated from the difference in dye concentration (mg/L) in the aqueous phase (C_o-$C_{e)}$ before and after adsorption respectively, using the equation given below:

$$\mathbf{q_e = \frac{(C_o - C_e)\,V}{m}} \quad \ldots\ldots (1)$$

Where Co and Ce (mg/L) are the initial and the equilibrium concentrations of dyes in the solution, V (L) is the volume of dye solution, m (g) is the mass of the used adsorbents in the experiment, and qe (mg/g) is the amount of adsorbed dyes per gram of adsorbents GO and GO-g-pBCM.

Adsorption Isotherms

There are various isotherm models to depict the isotherm results. In the present study, Langmuir and Freundlich's isotherm approaches are used to analyze the practical results [17]. Langmuir's approach [18] relies on the maximum adsorption that corresponds with the postulation of the liquid monolayer (adsorbate) on the solid (adsorbent) surface. The linearized type of Langmuir approach is shown below [19].

$$\mathbf{\frac{C_e}{q_e} = \frac{1}{(q_{max}.K_L)} + \frac{C_e}{q_{max}}} \quad \ldots\ldots (2)$$

Where C_e (mg/L) the BB dye equilibrium concentration; q_{max} (mg/g) the adsorption capacity required to complete monolayer on the adsorbent surface; q_e (mg/g) the amount of adsorbate per unit mass of adsorbent at equilibrium (mg/g); K_L Langmuir constant that relates to the energy of adsorption. Langmuir equation is valid for monolayer adsorption of the adsorbate onto the surface of the adsorbent and assumes there are restricted and homogenous adsorption sites. The fundamental attributes of a Langmuir model may be shown in terms of R_L [20] which is characterized by:

$$\mathbf{R_L = \frac{1}{1 + (K_L.C_e)}} \quad \ldots\ldots (3)$$

The other isotherm studied is Freundlich [21]; the general Freundlich isotherm experiential equation is given by [22]:

$$\mathbf{\ln q_e = \ln K_F + \frac{1}{n} \ln C_e} \quad \ldots\ldots (4)$$

Where K_F (L/mg) is adsorption constant and signifies the amount of adsorbed dye onto adsorbents at C_e, and 1/n is the empirical parameter correlated to the intensity of adsorption, and its value varies according to the heterogeneity of the adsorbent. A favorable adsorption process occurs with a value between 0 and 1 [23].

Adsorption Kinetics

Kinetics results benefit to describe dye uptake rates, which control the staying time of adsorbate at the solid-liquid interface and give helpful data for adsorption process designing. The exploratory kinetic curves can be assessed using various models. In this study, the appropriateness of pseudo-first-order and pseudo-second-order were examined to interpret the mechanism of BB dye adsorption onto GO and GO-g-BCM. The linear form of the kinetic model equations (5 and 6 respectively) can be expressed as [24]:

$$\mathbf{\ln q_e - q_t = \ln q_e - k_1 t} \quad \ldots\ldots (5)$$

$$\mathbf{\frac{t}{q_t} = \frac{1}{k_2.q_2^2} + \frac{t}{q_2}} \quad \ldots\ldots (6)$$

Where q_t and $q_{(1+2)}$ are the dye adsorbed amounts at time t and equilibrium respectively; k_1 is the adsorption rate constant of the pseudo-first-order model; k_2 is the adsorption rate constant of the pseudo-second-order model.

Thermodynamic Studies

Thermodynamic parameters can be determined from the thermodynamic equilibrium constant (K) or known as a thermodynamic distribution coefficient [25]. K is equal to:

$$\mathbf{K = \frac{C_a}{C_e}} \quad \ldots\ldots (7)$$

Where, Ca and Ce are the equilibrium concentrations of dye on the adsorbents (mg/g) and in the solution (mg/L), respectively. The data

of thermodynamic findings helpful to determine the change of standard enthalpy (ΔH°) and the change of standard entropy (ΔS°), that they can be calculated from the following equation [26]:

$$\ln K = \frac{\Delta S^{\circ}}{R} - \frac{\Delta H^{\circ}}{RT} \quad \ldots\ldots (8)$$

Where R is the universal gas constant (8.314 J/mol K), and T (K) is the absolute temperature, plotting of $\ln K_L$ versus 1/T leading to calculate ΔH° (kJ/mol) from the slope and ΔS° (J K^{-1} mol^{-1}) from the intercept. The standard Gibbs free energy ΔG° (kJ mol^{-1}) values were computed for each temperature used in adsorption processes from equation 9 [26].

$$\Delta G^{\circ} = \Delta H^{\circ} - T\Delta S^{\circ} \quad \ldots\ldots (9)$$

Results and Discussion:

Characterization of Adsorbents by Fourier-Transform Infrared Spectrometry (FTIR)

The presence of the additional functional groups on the modified graphene oxide GO surface is studied using FTIR spectroscopy. The spectrum of layer graphite powder is almost featureless, whereas that of GO (Fig. 2A) exhibits prominent bands at 3367 cm^{-1}, corresponds to hydroxyl stretching vibration, and at 1728 cm^{-1} corresponding to the stretching vibration of the carbonyl group (C=O), and the peak at 1620 cm^{-1} is attributed to aromatic C=C stretching vibrations. The FTIR spectra of GO and graphite are significantly different, where a high amount of oxygen-containing functional groups exist in the basal and edge planes of graphene oxide sheet[27], and the differences are generally proportionate to those that have been described previously [28], implying that graphene oxide was successfully prepared. The absorbance peaks of the GO-g-pBCM are observed at 1625, 1578, 1459, 1311, and 1160 cm^{-1} respectively as shown in Fig. 2B, combining those of GO and pBCM. Furthermore, the stretching vibration of the C=O peak shifts from 1728 cm^{-1} (GO) to 1625 cm^{-1} (GO-g-BCM), indicating interactions exist between GO and pBCM chains [29, 30].

Adsorption of BB Dyes onto GO and GO-g-pBCM

Adsorption experiments were run using the batch system technique for BB dye onto prepared adsorbents GO and GO-g-pBCM at optimum pH, contact time, and temperature.

Effect of pH

The pH of the dye solution plays a major role in the entire adsorption process, mainly on the adsorption capacity. The impact of pH on the adsorption capacities of prepared adsorbents was tested at the optimum initial concentration of BB dyes.

Figure 3 shows the pH effect on the adsorption capacities at different pH values ranging from 3.0 to 12.0 for BB dye after adsorption onto GO and GO-g-pBCM. The results achieved imply that the maximum pH of the adsorption process is dependent on the used adsorbate. Thus, the adsorption capacity seemed to be highly operative at pH 3.0 regardless of the nature of prepared adsorbents, where the q_{max} recorded at 708.5 mg g^{-1} for GO and 741.2 mg g^{-1} for GO-g-pBCM. So, a decrease in adsorption capacity occurred with increasing pH values, and consequently, a pH 3.0 value was chosen for the followed adsorption experiments. Notably, the surface of the adsorbents contains different functional groups such as carboxylic and hydroxyl groups. So, the change in pH values of dye solutions affects the ionization of these groups in GO and GO-g-pBCM adsorbent [31, 32], and the optimum pH for adsorption depends on the types of adsorbate and adsorbent [33].

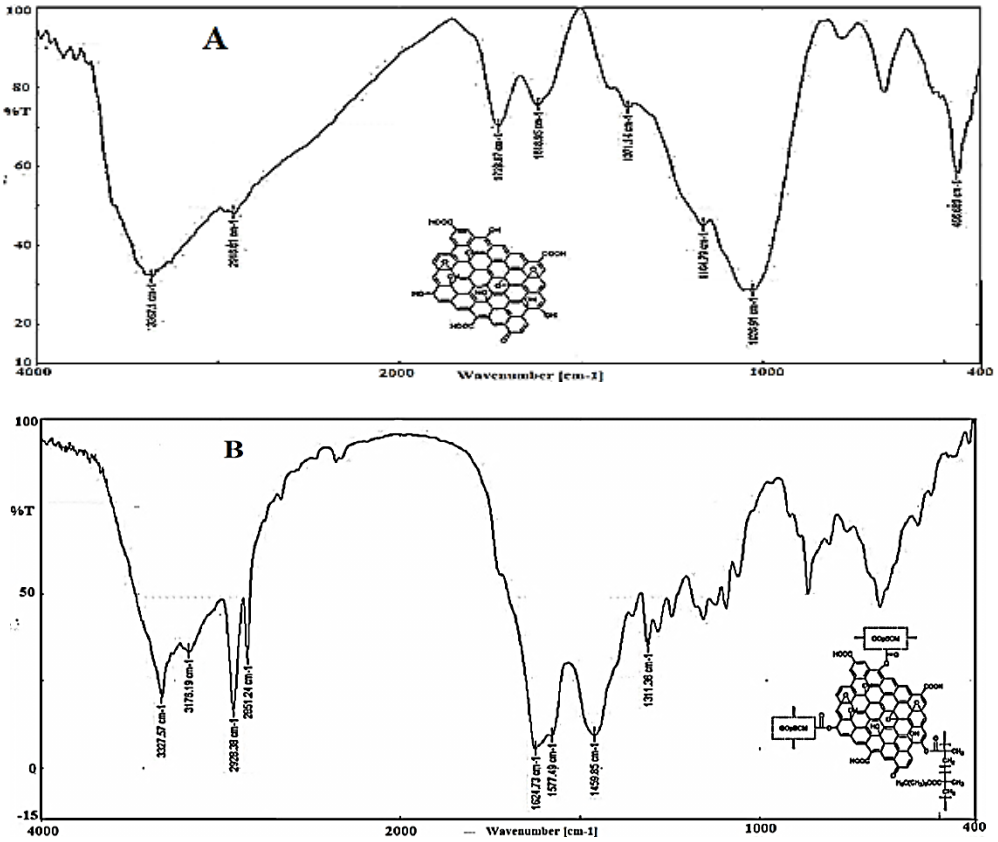

Figure 2. FTIR spectra of (A) GO and (B) GO-g-pBCM adsorbents.

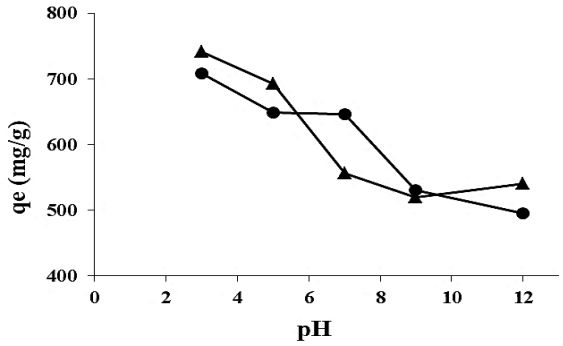

Figure 3. pH effect on the adsorption of BB dye on GO (●) and GO-g-pBCM (▲) at 27°C.

Effect of Contacting Time and Temperature

Figure 4 shows the influence of contacting time on the adsorption of BB at pH 3.0 onto adsorbents GO and GO-g-pBCM respectively, at different temperatures. Seemingly, from Fig. 4A, the adsorption of BB dye rapidly increased from (1-45 min), then the equilibrium was attained within (45-75 min) for adsorbent GO. While the behavior of BB dye adsorption by GO-g-pBCM as shown in Fig. 4B has rapidly increased from (1-15 min.), then the equilibrium was reached within (15-45 min.). Thus, the optimum agitation times for all further experiments were chosen as 45 min for adsorption of BB dye by adsorbent GO, and 15 min for the adsorbent GO-g-pBCM. Also, it is found that the adsorption capacity for GO and GO-g-pBCM increased as the temperature rose from 27°C to 60°C.

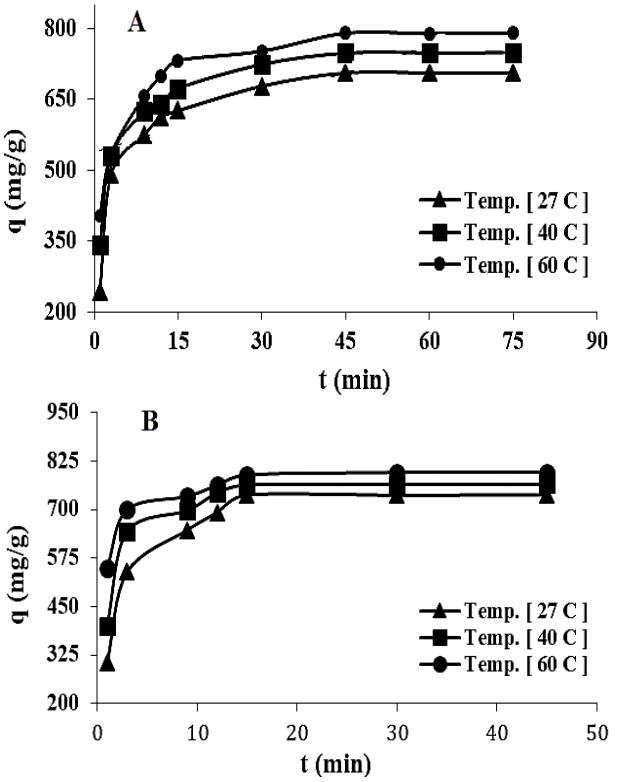

Figure 4. Agitation time effect of the BB dye adsorption onto (A) GO and (B) GO-g-pBCM at different temperatures.

Adsorption Isotherms

The isotherm data are fitted to different isotherm models to find the most reasonable model that can be used to explain the adsorption process. The Langmuir isotherm depends upon the higher limit of adsorption coincides with a monolayer saturated surface of adsorbent by adsorbate. When plotting C_e/q_e versus C_e, the slope of a plot equal to $(1/q_{max})$ and K_L can be calculated from the intercept. Figure 5A shows the plots of Langmuir adsorption isotherms and Fig. 5B shows the Freundlich adsorption isotherms of BB dye adsorbed onto prepared adsorbents GO and GO-g-pBCM, and their parameters and the correlation coefficient R^2 are given in Table 1.

The obtained R^2 for the Langmuir is closer to one than that of the Freundlich isotherm equation as shown in Table 1, and are arranging between $0.9987 \leq R^2 \leq 0.9992$. This describes a monolayer adsorption process onto a surface containing a finite number of adsorption sites on the prepared adsorbents. Also, R_L value for BB dye is less than one ($0.0194 \leq R_L \leq 0.0963$), which implies the favorability of the studied adsorbents for the adsorption process. This also suggests the creation of a BB monolayer on the GO and GO-g-pBCM adsorbent surface [34].

Table 1. Langmuir and Freundlich isotherm parameters for adsorption of BB dyes onto the prepared adsorbents at 27°C.

Adsorbent	Langmuir Isotherm				Freundlich Isotherm		
	q_m	K_L	R_L	R^2	K_F	1/n	R^2
GO	833.3	0.1263	0.0194	0.9988	527.15	0.0772	0.9004
GO-g-pBCM	1000	0.0900	0.0270	0.9989	451.91	0.1407	0.9882

K_L: (L/mg), q_{max}: (mg/g)

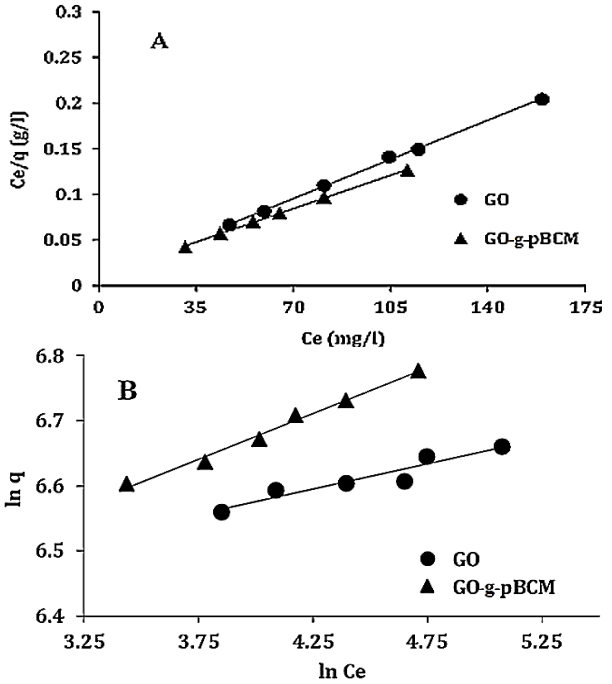

Figure 5. Langmuir (A) and Freundlich (B) adsorption isotherms of BB dye onto GO and GO-g-pBCM adsorbents at 27℃.

Kinetic Study

Two kinetic models were tested to explain the adsorption mechanism of BB dyes onto GO and GO-g-pBCM. The first model was the pseudo-first-order. Plotting of ln (q_e-q_t) against t (according to eq. 5) will result in a straight line of the slope of k_1 and intercept of ln (qe). Figure 6 exhibits the pseudo-first-order equations for adsorption BB dye onto adsorbents GO and GO-g-pBCM respectively at temperatures 27, 40, and 60℃. The second kinetic model was pseudo-second-order. The q_2 and k_2 are determined from the plot of t/q_t versus t (according to equation 6) from the slope and intercept, respectively. They are displayed in Fig. 7 for the adsorption of BB dye onto GO and GO-g-pBCM at different temperatures (27, 40, and 60℃). All results obtained are summarized in Table 2.

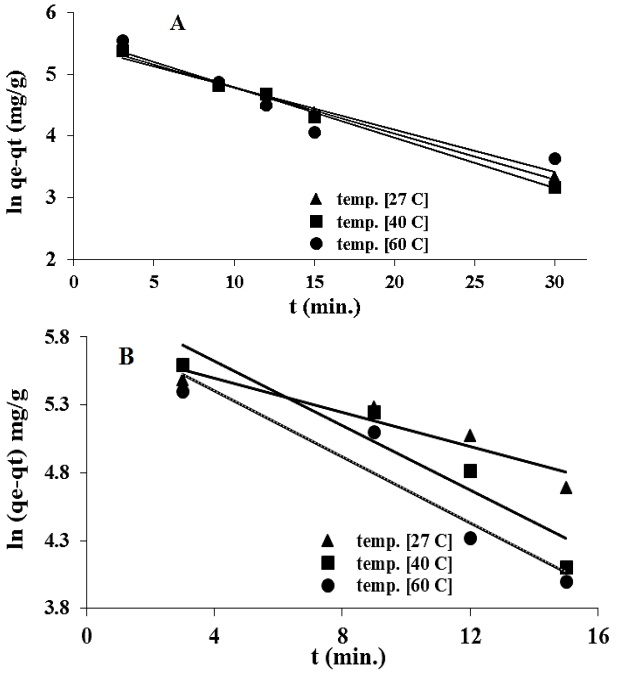

Figure 6. Pseudo-first-order plots for the adsorption of BB dye onto (A) GO and (B) GO-g-pBCM at different temperatures.

Table 2. Kinetic parameters for adsorption of BB dye onto prepared adsorbents at different temperatures

Adsorbent	Temp. (°C)	Pseudo-first-order			Pseudo-second-order		
		k_1	q_1	R_1^2	k_2	q_2	R_2^2
GO	27	0.074	251.36	0.9922	0.00065	714.28	0.9992
	40	0.081	251.36	0.9960	0.00063	769.23	0.9993
	60	0.067	235.61	0.8633	0.00060	833.33	0.9993
GO-g-pBCM	27	0.062	312.93	0.8962	0.00069	8333.33	0.9967
	40	0.118	445.23	0.8928	0.00120	8333.33	0.9983
	60	0.121	361.83	0.9039	0.00280	714.286	0.9986

k_1: (min^{-1}), q: (mg/g), k_2: (g mg^{-1} min^{-1})

The R^2 values from two kinetics models for BB dye adsorption are $R^2 \leq 0.9960$ and $R^2 \leq 0.9993$ for the pseudo-first-order and pseudo-second-order respectively. Furthermore, the calculated q_{max} is highly effective with the experimental data. This suggests that the kinetic modeling of the temperature effect is more likely to fit the model of the pseudo-second-order adsorption [35].

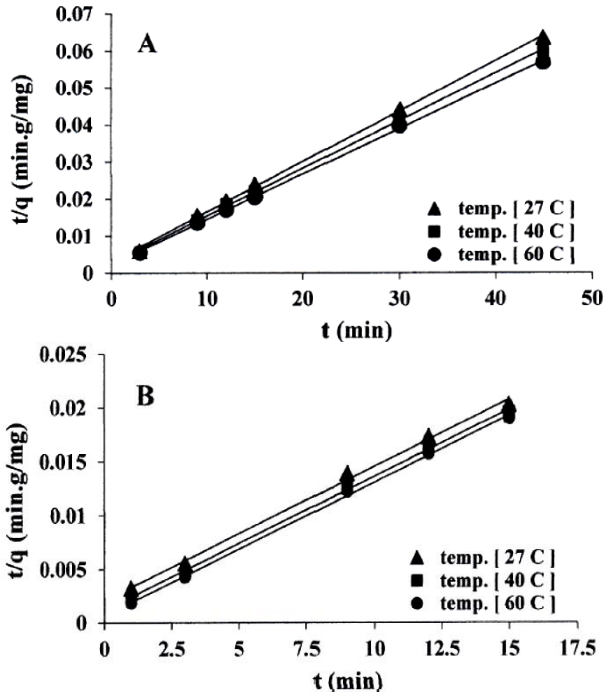

Figure 7. Pseudo-second-order plots for the adsorption of BB dye onto GO (A) and GO-g-pBCM (B) at different temperatures.

Thermodynamic Study

The enthalpy, entropy, and the free energy changes for the adsorption of BB dye onto GO and GO-g-pBCM are calculated as per the equilibrium data, and their values are shown in Table 3 and Fig. 8 demonstrates the ΔH° and ΔS° for adsorption of BB dye onto GO and GO-g-pBCM respectively. At all studied temperatures, ΔG° was negative implying that the adsorption process is spontaneous and reflecting the affinity of adsorbents towards BB dye[36]. The positive value of ΔH° verifies the endothermic character of the adsorption, also the positive value of ΔS° explains the increase of the adsorption process randomness and affinity of the adsorbents for BB dye [37].

Table 3. Thermodynamic parameters for adsorption of BB dye onto adsorbents at different temperatures.

Adsorbent	Temp.	K	ΔH°	ΔS°	ΔG°
GO	300.15	7.5	60.175	216.172	-4.709
	313.15	14.3			-7.519
	333.15	79.0			-11.843
GO-g-pBCM	300.15	11.8	46.857	176.066	-5.988
	313.15	21.1			-8.277
	333.15	74.7			-11.799

Temp: (K), ΔH°, ΔG° (kJ mol^{-1}), ΔS°: (J K^{-1} mol^{-1})

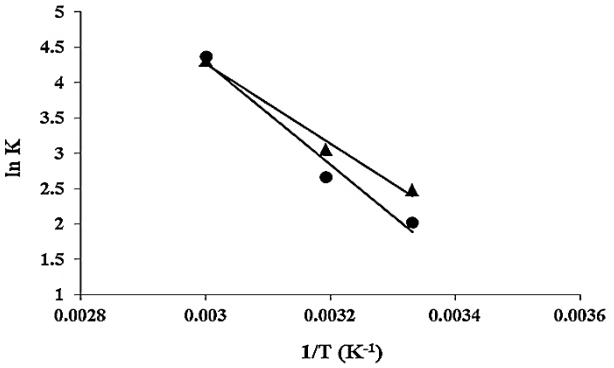

Figure 8. Plots of lnK vs. 1/T for the estimation of thermodynamic parameters for the adsorption of BB dye onto GO (●) and GO-g-pBCM (▲).

Conclusions:

In this work, GO and GO-g-pBCM synthesized based on graphite were investigated to evaluate the removing applicability of BB dye from the aqueous solutions. The highest adsorption occurred to BB dye with pH 3.0 for both adsorbents GO and GO-g-pBCM. It is found that the maximum adsorption capacity, q_{max}, values are 833.3 and 1111.1 mg/g for BB dye adsorbed onto GO and GO-g-pBCM respectively. Depending on the R^2 values, the pseudo-second-order model accurately expressed

the adsorption kinetics of the BB dye onto both adsorbents. Thermodynamic parameters showed that the spontaneous nature of adsorption systems of the adsorbents and confirm the endothermic nature of the adsorption.

Authors' declaration:

- Conflicts of Interest: None.
- We hereby confirm that all the Figures and Tables in the manuscript are mine. Besides, the Figures and images, which are not mine ours, have been given permission for re-publication attached with the manuscript.
- Ethical Clearance: The local ethical committee at University of Basrah approved the project.

Authors' contributions statement:

Hadi S. Al-Lami and Ali A. Abdulwahid suggested and planned the current research idea. Alaa A. Mizhr designed and carried out the experiments. All authors contributed in the analysis and discussing of the results and writing the manuscript.

References

1. Shahabuddin S, Khanam R, Khalid M, Sarih NM, Ching JJ, Mohamad S, et al. Synthesis of 2D boron nitride doped polyaniline hybrid nanocomposites for photocatalytic degradation of carcinogenic dyes from aqueous solution. Arabian J. Chem. 2018;11:1000-16.
2. Zhou X, Zheng P, Wang L, Liu X. Preparation of sulfonated poly (arylene ether nitrile)-based adsorbent as a highly selective and efficient adsorbent for cationic dyes. Polymers. 2019;1(1):1-17.
3. Fatima B, Siddiqui SI, Ahmed R, Chaudhry SA. Green synthesis of f-CdWO4 for photocatalytic degradation and adsorptive removal of Bismarck Brown R dye from water. Water Resour. Ind. 2019;22:1-18.
4. Siddiqui SI, Rathi G, Chaudhry SA. Acid washed black cumin seed powder preparation for adsorption of methylene blue dye from aqueous solution: thermodynamic, kinetic and isotherm studies. J. Mol. Liq. 2018;264:275-84.
5. Sherino B, Abdul Halim SN, Shahabuddin S, Mohamad S. Simultaneous removal of carcinogenic anionic and cationic dyes from environmental water using a new Zn-based metal-organic framework. Sep. Sci. Technol. 2020:1-4.
6. Wu Sk, Pan Y, Wang N, Lu T, Dai W j. Azo dye degradation behaviour of AlFeMnTiM (M= Cr, Co, Ni) high-entropy alloys, Int. J. Miner. Metall. Mater. Metallurgy, and Materials. 2019;26:124-32.
7. Kim S, Park CM, Jang M, Son A, Her N, Yu M, et al. Aqueous removal of inorganic and organic contaminants by graphene-based nano adsorbents: A review. Chemosphere. 2018;212:1104-24.
8. Ai Y, Liu Y, Lan W, Jin J, Xing J, Zou Y,et al. The effect of pH on the U (VI) sorption on graphene oxide (GO): a theoretical study. Chem. Eng. J. 2018;343:460-6.
9. Guo L, Xu Y, Zhuo M, Liu L, Xu Q, Wang L, et al. Highly efficient removal of Gd (III) using hybrid hydrosols of carbon nanotubes/graphene oxide in dialysis bags and synergistic enhancement effect. Chem. Eng. J. 2018;348:535-45.
10. Yang Y, Yu Y, Yang N, Huang B, Kuang YF, Liao YW. Adsorption behaviour of isocyanate/ethylenediaminetetraacetic acid-functionalized graphene oxides for Cu^{2+} removal. Water Sci. Technol. 2018;78:2459-68.
11. Zhang J, Azam MS, Shi C, Huang J, Yan B, Liu Q, et al. Poly (acrylic acid) functionalized magnetic graphene oxide nanocomposite for removal of methylene blue, RSC Advances. 2015;5:32272-82.
12. Mizhir AA, Abdulwahid AA, Al-Lami HS. Chemical functionalization graphene oxide for the adsorption behaviour of Bismarck Brown dye from aqueous solutions. Egypt. J. Chem. 2020;63(5):1679-1696.
13. Islamova RM, Golovochesova OI, Monakov YB, Utepova IA, Musikhina AA, Chupakhin ON. Effect of heterocyclic derivatives of ferrocene on free-radical polymerization of methyl methacrylate and styrene. Polym. Sci. Ser. B 2010;52(11-12):637-47.
14. Yakimtsova LB, Egorova EL, Matusevich YI, Selevich KA, Kurtikova AL. Preparation and thermal degradation of methyl methacrylate-methacrylic acid copolymers. Russ. J. Appl. Chem. 2009;82(9):1636-43..
15. Liu J, Liu G, Liu W. Preparation of water-soluble β-cyclodextrin/poly (acrylic acid)/graphene oxide nanocomposites as new adsorbents to remove cationic dyes from aqueous solutions. Chem. Eng. J. 2014;257:299-308..
16. Sabnis RW. Handbook of biological dyes and stains: synthesis and industrial applications, John Wiley & Sons. USA 2010.
17. Fraga TJM, de Souza ZSB, Fraga DM, Carvalho MN, de Luna Freire EMP, Ghislandi MG, et al. Comparative approach towards the adsorption of Reactive Black 5 and methylene blue by n-layer graphene oxide and its amino-functionalized derivative. Adsorption. 26 (2020) 283-01.
18. Langmuir I. The adsorption of gases on plane surface of glass, mica and platinum, J. Am. Chem. Soc. 1918;40:1361-403.
19. Hasanzadeh M, Simchi A, Far HS. Nanoporous composites of activated carbon-metal organic frameworks for organic dye adsorption: Synthesis, adsorption mechanism and kinetics studies. J. Ind. Eng. Chem. 2020;81:405-14.
20. Sultan MT, Al-Lami HS, Al-Dujiali AH. Synthesis and characterization of alumina-grafted acrylic acid monomer and polymer and its adsorption of phenol and p-chlorophenol. Desalin. Water Treat. 2019;150:192-03.
21. Freundlich HMF. About the adsorption. Zeitschrift für Physikalische Chemie, 1906;57:385–470.
22. Wang G, Zhang Z, Li W, Du C, Chen T. Production and characterization of modified biochar by corn cob and its ability to absorb phenol. In IOP Conference

Series: Mater. Sci. Eng. 2020 (Vol. 729, No. 1, p. 012070). IOP Publishing.
23. Senturk HB, Ozdes D, Gundogdu A, Duran C, Mustafa S. Removal of phenol from aqueous solutions by adsorption onto organomodified Tirebolu bentonite: Equilibrium, kinetic and thermodynamic study, J. Hazard. Mater. 2009; 172:353–362.
24. Potgieter JH, Pearson S, Pardesi C. Kinetic and Thermodynamic Parameters for the Adsorption of Methylene Blue Using Fly Ash under Batch, Column, and Heap Leaching Configurations. Coal Combustion and Gasification Products. 2018;10(2):23-33.
25. Bu J, Yuan L, Zhang N, Liu D, Meng Y, Peng X. High-efficiency adsorption of methylene blue dye from wastewater by a thiosemicarbazide functionalized graphene oxide composite. Diamond Relat. Mater. 2020;101:1-10.
26. Goddeti SM, Bhaumik M, Maity A, Ray SS. Removal of Congo red from aqueous solution by adsorption using gum ghatti and acrylamide graft copolymer coated with zero valent iron. Int. J. Biol. Macromol. 2020;149:21-30.
27. Zhong M, Liu YT, Xie XM. Self-healable, super-tough graphene oxide–poly (acrylic acid) nanocomposite hydrogels facilitated by dual cross-linking effects through dynamic ionic interactions. J. Mater. Chem. B . 2015;3(19):4001-8.
28. Ma J, Cai P, Qi W, Kong D, Wang H. The layer-by-layer assembly of polyelectrolyte functionalized graphene sheets: a potential tool for biosensing. Colloids Surf. A Physicochem. Eng. Asp. 2013;426:6-11.
29. Park S, Lee KS, Bozoklu G, Cai W, Nguyen ST, Ruoff RS. Graphene oxide papers modified by divalent ions enhancing mechanical properties via chemical cross-linking. Am. Chem. Soc. Nano. 2020;(2):572-78.
30. Cong HP, Wang P, Yu SH. Highly elastic and super stretchable graphene oxide/polyacrylamide hydrogels. Small. 2014; 10:448-53.
31. Jain R, Shrivastava M. Adsorptive studies of hazardous dye Tropaeoline 000 from an aqueous phase on to coconut-husk. J. Hazard. Mater. 2008;158(2-3):549-56.
32. Bazrafshan E, Mostafapour FK, Hosseini AR, Khorshid AR, Mahvi AH. Decolourization of reactive red 120 dye by using single-walled carbon nanotubes in aqueous solutions, J. Chem. 2013;1-8.
33. Zhang L, Zeng Y, Cheng Z. Removal of heavy metal ions using chitosan and modified chitosan: A review, J. Mol. Liq. 2016,;214:175-191.
34. Gilles CH, Macewan TH, Nakhwa SN, Smith D. A system of classification of solution adsorption isotherms, and its use in diagnosis of adsorption mechanisms and measurement of specific surface areas of solids. J. Chem. Soc. 1960;2:3973-93.
35. Islam M, Mishra PC, Patel R. Fluoride adsorption from aqueous solution by a hybrid thorium phosphate composite. Chem. Eng. J. 2011;166(3):978-85.
36. Ren S, Meng Z, Sun X, Lu H, Zhang M, Lahori AH, et al. Comparison of Cd2+ adsorption onto amphoteric, amphoteric-cationic and amphoteric-anionic modified magnetic bentonites, Chemosphere. 2020;239:124840.
37. Tran HN, Tomul F, Nguyen HTH, Nguyen DT, Lima EC, Le GT. Innovative spherical biochar for pharmaceutical removal from water: Insight into adsorption mechanism. J. Hazard. Mater. 2020; 394:1-46.

دراسة حركية وثرموديناميكة لإمتزاز صبغة بسمارك البنية على أكسيد الكرافين وأكسيد الكرافين-المطعم ببولي (ن-بيوتيل ميثاكريلات-مشترك-حامض ميثاكريليك)

علاء عادل مزهر[1] **هادي سلمان اللامي[2]** **علي عبدالرزاق عبدالواحد[2]**

[1]قسم علوم البحار التطبيقية ، كلية علوم البحار ، جامعة البصرة
[2]قسم علوم الكيمياء، كلية العلوم، جامعة البصرة

الخلاصة:

تم دراسة سلوك إمتزاز صبغة بسمارك البنية BB من المحاليل المائية على أوكسيد الكرافين GO وأكسيد الجرافين–مطعم-بولي(ن-بيوتيل ميثاكريلات-مشترك-حامض ميثاكريليك) GO-g-pBCM المحضرين. تم تشخيص الممتزات المحضرة بمطيافية الأشعة تحت الحمراء FTIR التي أكدت صحة التراكيب الممتزات المحضرة. تم دراسة أمتزاز الصبغة بصيغتي لانكمير وفرندليش على أوكسيد الكرافين وأكسيد الجرافين –مطعم-بولي (ن-بيوتيل ميثاكريلات-مشترك- حامض ميثاكريليك) في سلسلة من التجارب بنظام الوجبة وتحت ظروف مختلفة. واعتُبر نموذج لانگماير معقولاً على نحو متزايد من المعلومات التجريبية لإمتزاز الصبغة. وكشفت الدراسة الحركية أن نموذج النظام الثاني الكاذب أظهر أفضل ملائمة للبيانات التجريبية، وأن المعاملات الحرارية تعني أن عملية الامتزاز كانت تلقائية ومن النوع الماص للحرارة.

الكلمات المفتاحية: ايزوثيرم الإمتزاز، صبغة بسمارك البنية، فريندليش، أوكسيد الكرافين، لانگماير، نموذج من الدرجة الثانية الكاذبة